

Measurements of strain and the optical indices in the ferroelectric $\text{Ba}_{0.4}\text{Sr}_{0.6}\text{Nb}_2\text{O}_6$: Polarization effects

A. S. Bhalla, R. Guo, and L. E. Cross

Materials Research Laboratory, The Pennsylvania State University, University Park, Pennsylvania 16802

Gerald Burns and F. H. Dacol

IBM Thomas J. Watson Research Center, P.O. Box 218, Yorktown Heights, New York 10598

Ratnakar R. Neurgaonkar

Rockwell International Science Center, Thousand Oaks, California 91360

(Received 17 November 1986)

We report accurate temperature-dependent measurements of the optic index of refraction, the birefringence, and the strain in the ferroelectric, tungsten-bronze crystal $\text{Ba}_{0.4}\text{Sr}_{0.6}\text{Nb}_2\text{O}_6$. This composition congruently melts, so large homogeneous high-quality crystals can be grown. From the experimental data, it appears that far above the ferroelectric phase transition temperature ($T_c \approx 88^\circ\text{C}$), up to a temperature T_d ($\approx 300^\circ\text{C}$), the crystals appear to possess a local, randomly oriented (up or down), polarization P_d . The values of T_d obtained from the index and completely independent strain measurements are in very good agreement with each other, as are the values of P_d . Various aspects of our understanding of the polarization behavior and other effects in this ferroelectric system are discussed.

INTRODUCTION

There is a great deal of interest in ferroelectric materials that have the tungsten-bronze crystal structure.¹ Above the ferroelectric transition temperature T_c , the structure is tetragonal and has a center of symmetry (space group $D_{4h}^5-P_{4/mbm}$).² Below T_c it remains tetragonal ($C_{4v}^2-P_{4bm}$) with a reversible spontaneous polarization P_r , along the tetragonal or c axis. These space groups refer to the average crystal structure (these are defect structures^{2,3}) and will be discussed below; none of the tungsten-bronze ferroelectrics actually are ordered compounds.⁴

In this paper the properties of the tungsten-bronze ferroelectric $\text{Ba}_{1-x}\text{Sr}_x\text{Nb}_2\text{O}_6$ (BSN) are discussed. It has been shown that for $x \approx 0.6$ the material is congruently melting⁵ and, hence, large crystals of high optical quality can be grown,⁶ which have found many applications.⁷ The primitive unit cell of this material is shown in Fig. 1. The chemical formula can be usefully thought of as

$(\text{Ba}_{1-x}\text{Sr}_x)_5(\text{NbO}_3)_{10}$ since there are ten niobium octahedra in this unit cell and the Ba and Sr atoms occupy the α and β positions randomly. However, there are six such positions and only five Ba+Sr atoms; thus the structure has built-in defects.

Recently, there has been considerable discussion of "crystalline ferroelectrics [specifically the tungsten-bronze ferroelectric $\text{K}_2\text{Sr}_4(\text{NbO}_3)_{10}$] with a glassy polarization phase."⁸⁻¹⁰ These are materials in which there is evidence for regions of local, randomly oriented, polarization far above the ferroelectric transition temperature T_c , up to a temperature T_d . The principal evidence for this behavior comes from the temperature dependence of the index of refraction, $n(T)$. However, there is now evidence from low-temperature thermal-conductivity and specific-heat measurements,¹¹ Raman measurements of the phonon spectra,¹² and second-harmonic-generation measurements¹³ for the existence of such polarization behavior. Some aspects of this work have been reviewed.¹⁴

In this paper, for BSN we show that measurements of the temperature dependence of the length, that is, strain, $x(T)$, also gives strong evidence for a polarization far above T_c . Further, the strain and index measurements, on the same samples, lead to consistent results. In a discussion, at the end of the paper, we relate these crystalline ferroelectrics that have an extended polarization behavior above the dielectric maximum to ferroelectrics with a diffuse phase transition.

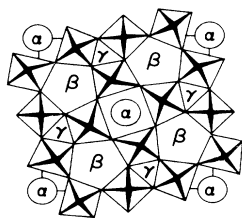


FIG. 1. The unit cell of the tungsten bronze $(\text{Ba,Sr})_5(\text{NbO}_3)_{10}$ looking down the c axis.

EXPERIMENTAL

Large, clear optical-quality BSN crystals were pulled from the melt by the Czochralski technique in a manner

described previously.⁶ The earlier problems of coring and striations in growing tungsten-bronze ferroelectrics have been eliminated by using very pure starting materials and pulling at the congruent melting composition.^{5,6} Before use, all samples were annealed overnight at 500°C in order to remove internal stresses and possible bias effects.

The remanent polarization P_r was obtained by the integration of the pyroelectric-coefficient-versus-temperature method.¹⁵ Thin, sputtered gold c plates were used, and the samples were cooled through the transition temperature ($T_c \approx 88^\circ\text{C}$) with a dc field of 10 kV/cm. The dielectric constant was measured by standard techniques.

The index of refraction parallel to P_r (n_3) and perpendicular to P_r (n_1) were measured by the minimum-deviation technique.⁸ Oriented BSN prisms were used in an oven in conjunction with various lasers as light sources.

The birefringence, Δn_{31} , was also directly measured. An a -cut plate (i.e., the a axis perpendicular to the plate) was polished into a wedge shape with a known wedge angle (5° – 7°). Δn_{31} was measured using a polarizing microscope with a hot stage and the sodium D lines as a light source ($\lambda = 5893 \text{ \AA}$). The birefringence was determined by

$$\Delta n_{31} = \lambda/d \sin\theta, \quad (1)$$

where θ is the wedge angle and d is the separation between the interference fringes resulting from the varying thickness of the wedge.

The length measurements were made from room temperature to 500°C under a heating rate of 1°C/min on rectangular bar BSN samples cut normal to the c axis to give $x_3(T)$, or the a axis, to give $x_1(T)$, typically 8 mm \times 1 mm \times 1 mm. The strains were measured as a function of temperature using a linear voltage-differential transformer (LVDT) dilatometer (model 24DCDT-250 or model 24DCDT-050) from the Schwartz Co., N.J.

RESULTS

Polarization

The temperature dependence of the dielectric constant along the ferroelectric axis, $\epsilon_3(T)$, the reversible spontaneous polarization P_r , and the pyroelectric coefficient are plotted in Fig. 2. The results are in reasonable agreement with earlier published data on these materials.^{1,16} From $\epsilon_3(T)$ we see that $T_c \approx 88^\circ\text{C}$ and note that P_r is down to zero by $\approx 100^\circ\text{C}$. This behavior is in sharp contrast to the fluctuating polarization behavior that will be discussed later.

$n(T)$ and $x(T)$ theory

We consider the macroscopic quantities, the change of the optic index of refraction, $n(T)$, and the strain, $x(T)$, which is the fractional change of length. In a centrosymmetric crystal, by symmetry both of these quantities depend on the square of the polarization in the same way:

$$\Delta(n^{-2})_{ij} = \sum_{k,l} g_{ijkl} P_k P_l, \quad (2)$$

$$x_{ij} = \sum_{k,l} Q_{ijkl} P_k P_l, \quad (3)$$

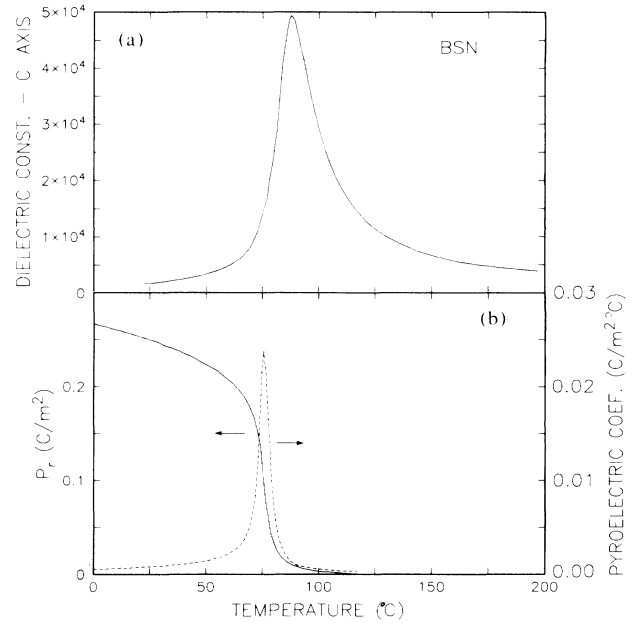


FIG. 2. The measured temperature dependence of the dielectric constant (ϵ), reversible spontaneous polarization (P_r), and the pyroelectric coefficient.

where g and Q are the quadratic electro-optic and electrostrictive coefficients, respectively (both fourth-rank tensors). The subscripts can have values 1, 2, or 3 for the three directions (x , y , and z), and P is the polarization. Since BSN is tetragonal, both above and below T_c it is easy to write the tensor effects parallel (3 component) and perpendicular (1 component) to the tetragonal axis (3 axis or z axis). Assuming that all polarization must occur along the ferroelectric (3) axis, then in contracted notation^{3,17} we have, for the indices of refraction,

$$\Delta n_3 = -g_{33}(n_3^0)^3 P_3^2 / 2, \quad (4a)$$

$$\Delta n_1 = -g_{13}(n_1^0)^3 P_3^2 / 2, \quad (4b)$$

and for the birefringence,

$$\delta(\Delta n_{31}) \equiv \Delta n_3 - \Delta n_1 = -\frac{1}{2}(n_3^0)^3 \left[g_{33} - g_{13} \left(\frac{n_1^0}{n_3^0} \right)^3 \right] P_3^2, \quad (4c)$$

where n^0 is the index of refraction if there were no polarization of any sort present, whether along the 3 axis (n_3^0) or perpendicular to it (n_1^0).

For the strains the expression are

$$\Delta c/c_0 = Q_{33} P_3^2, \quad (5a)$$

$$\Delta a/a_0 = Q_{13} P_3^2. \quad (5b)$$

An important aspect of Eqs. (4) and (5) is that they depend quadratically on the polarization. Thus, if P_3 is randomly, spatially directed up and down, the effects will

add, not cancel. The second important point to appreciate is that P_3 can be spatially inhomogeneous, but still the effects will add. For measurements of the crystal lengths this is clear. For $n(T)$ measurements the spatial resolution is of the order of the wavelength of light; thus local polarization regions that can be several thousand angstroms apart will be effectively averaged.

$n(T)$ data

Figure 3(a) shows the indices of refraction both parallel and perpendicular to the tetragonal c axis at 6328 Å. As can be seen, the changes in n_3 are considerably larger than those perpendicular to the tetragonal axis (n_1), which is shown in Fig. 3(b) on a considerably expanded scale. These data are similar to those published previously.^{18,10} The most noticeable difference between these results and the earlier data¹⁸ is the lack of thermal hysteresis near T_c . The reason for this is not totally clear; however, the crystals reported on here are very pure, annealed, and were grown at the congruent point in the phase diagram, which results in striation-free crystals. Thus we believe that these crystals represent the true behavior.

Measurements taken at 6328 and 4880 Å for n_3 are plotted in Fig. 4, where a constant has been subtracted from the latter results so that both can be presented on the same expanded scale.

The data for n_3 at 6328 Å are the same as shown in Fig. 3. Classical, soft-mode ferroelectrics have an index of refraction that is approximately linear with temperature

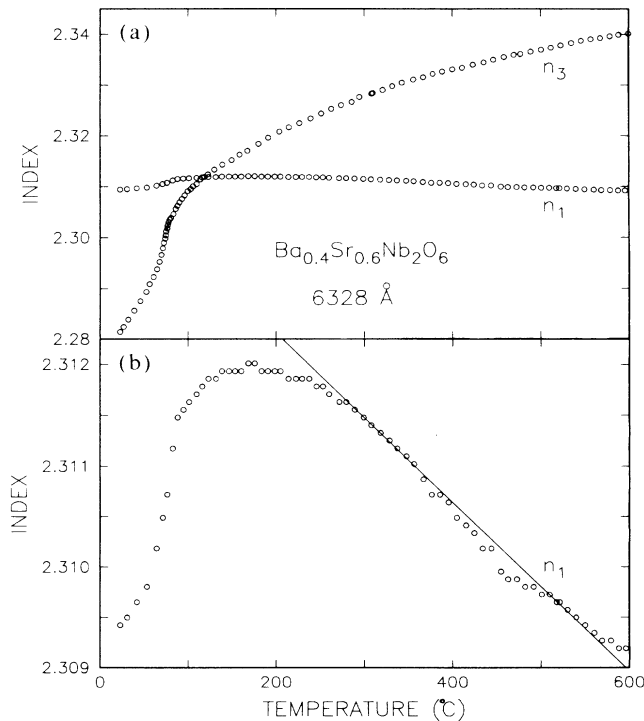


FIG. 3. (a) The measured n_3 and n_1 at 6328 Å. (b) The same n_1 shown on an expanded scale.

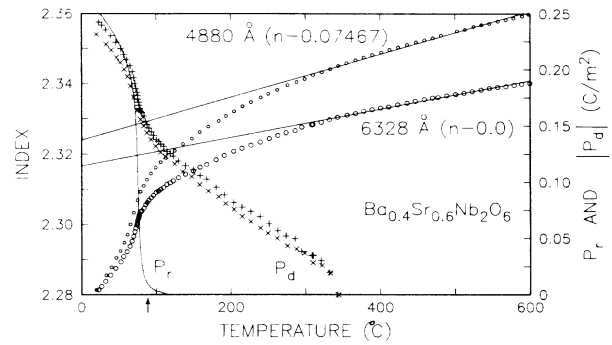


FIG. 4. The temperature dependence of n_3 at two wavelengths as indicated. P_d obtained, as described in the text, is shown. Also shown in P_r obtained from Fig. 2.

above T_c ; then below T_c , $n(T)$ reflects the spontaneous polarization via Eq. 4(a). Such behavior has been reported in several systems.¹⁹ However, the data in Fig. 4 behave quite differently. There is no linear behavior just above T_c ; instead, there appears to be considerable curvature in n_3 above T_c .

The two straight lines in Fig. 4 approximately represent the high-temperature linear behavior of $n_3(T)$. T_d is functionally defined as the temperature at which the straight line deviates from the measured data. As can be seen, for the data taken at both wavelengths, approximately the same values of T_d are found. Assuming that the deviations from the straight-line behavior are due to local polarization regions, the data can be analyzed via Eq. 4(a) to yield a polarization, which is called P_d . This procedure has been used before.⁷⁻¹⁰ To analyze the data in this manner [via Eq. 4(a)], for each wavelength the straight line is taken as n^0 , Δn is the difference between the straight line and the measured values (Δn is zero at T_d), and, as used before,¹⁰ we take $g_{33} = 0.10$ and $0.12 \text{ m}^4/\text{C}^2$ at 6328 and 4880 Å, respectively.²⁰⁻²² The resultant values of P_d at the two wavelengths are plotted in Fig. 4. The use of the small wavelength dependence²¹ of g_{33} improves the agreement between the two sets of data, which gives some indication that the ideas in this approach of analysis is correct. Also shown in Fig. 4 is the reversible polarization from Fig. 2. As can be seen, P_r and P_d are in reasonable agreement at room temperature, which again indicates that our understanding, via the quadratic electro-optic effects, is appropriate.

Figure 5 shows birefringence, Δn_{31} , as a function of temperature. BSN is an optically negative crystal. As is evident from Fig. 5, Δn_{31} decreases with temperature and goes through zero above T_c and the crystal becomes optically positive. Similar to the n_3 and n_1 -versus- T data [Fig. 3(a)], there is no thermal hysteresis noticed in the Δn_{31} -versus- T data. Also shown in this figure is $n_3 - n_1$ obtained (via Fig. 3) at 6328 Å. The results are in very good agreement with Δn_{31} , which was measured at 5893 Å. From these data, P_d can be obtained as has been discussed above with respect to $n_3(T)$. To do this, we used a value of $0.09 \text{ m}^4/\text{C}^2$ for the average value of g_{ij} , the term

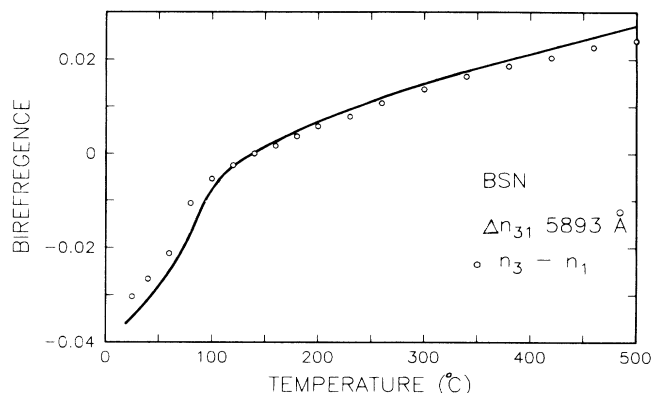


FIG. 5. The solid line is the birefringence (Δn_{31}) measured with the sodium D lines. The results for heating and cooling overlap each other. The open circles are $n_3 - n_1$ obtained from the measurements in Fig. 3.

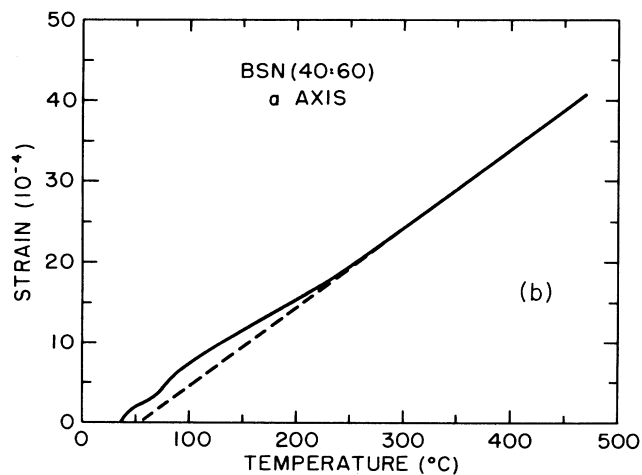
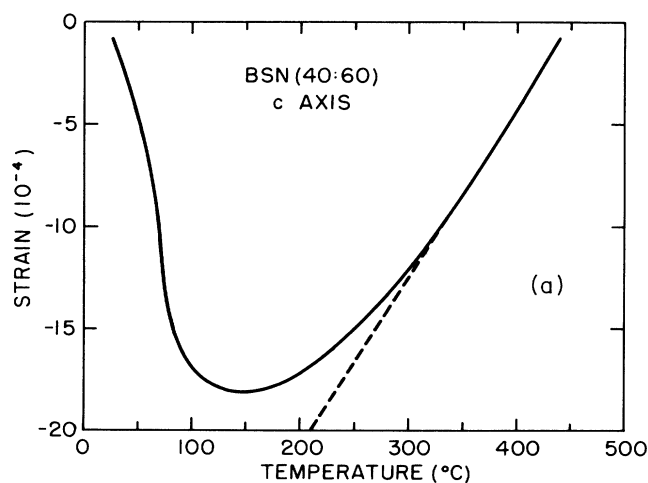


FIG. 6. (a) The measured strain along the c axis obtained as described in the text. (b) The same, but perpendicular to the c axis.

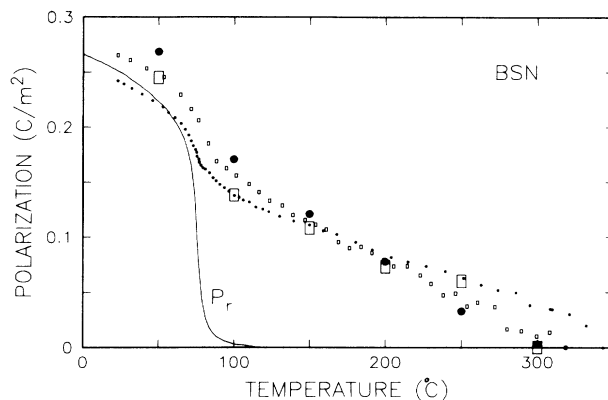


FIG. 7. Values of P_d , obtained by the different methods are summarized in this figure. Also, the reversible, spontaneous polarization P_r is shown as the solid line. P_d obtained from n_3 are given by the small circles, values from n_1 are given by the small open rectangles, values from the birefringence n_{31} are given by the large open rectangles, and values from $\Delta c/c$ are given by the large solid circles.

in large square brackets in Fig. 4(c). These results will be presented and discussed in connection with the last figure.

$x(T)$ data

The thermal strain parallel ($\Delta c/c$) and perpendicular ($\Delta a/a$) to the ferroelectric c axis have been measured by a high-sensitivity dilatometer. The results are shown in Figs. 6(a) and 6(b), respectively. The highest-temperature data, far above T_c , can be approximated by a straight line, along both axes, as can be seen in the figures. The deviation from this linear high-temperature behavior occurs at approximately the same temperature ($\approx 300^\circ\text{C}$). However, due to the much larger strain along the c axis, we place more emphasis on these data than those perpendicular to the c axis. (The same situation occurs for index data, see Figs. 3 and 4.)

We analyze the deviation of the strain from the high-temperature linear behavior via Eq. 5(a) to obtain P_d . Using the measured $\Delta c/c$ and a value²³ of $Q_{33} = 3 \times 10^{-2} \text{ m}^4/\text{C}^2$, then P_d can be calculated. The results are plotted in Fig. 7.

DISCUSSION

In Fig. 7 we summarize the P_d , really $(\bar{P}_d^2)^{1/2}$, values obtained from n_3 , Δn_{31} , $\Delta c/c$, and even n_1 , which was not discussed as yet. Also plotted is the normal reversible polarization data, P_r , from Fig. 2.

Considering the differences between the physical quantities that are measured (various aspects of the optic index of refraction and strain), the agreement in the P_d values in Fig. 7 is excellent. The values are in good agreement not only in magnitude but also in the T_d values (the temperature at which P_d differs from zero).

Good agreement would be expected for P_d obtained from $n_3(T)$ and $\Delta n_{31}(T)$ since the largest variations with

temperature come from n_3 (Fig. 2). However, it is reassuring to see that this is the case, remembering that the measuring techniques are quite different. Also plotted in Fig. 7 is P_d obtained from $n_1(T)$. As can be seen in Fig. 3(a), the temperature variation of n_1 is small compared to n_3 , yet the data are sufficiently accurate so that a reasonable high-temperature linear region can be delineated [the straight line in Fig. 3(b)] and P_d can be calculated [via Eq. 4(b)] using $g_{13} = 0.01 \text{ m}^4/\text{C}^2$, as discussed. The results are quite consistent with P_d obtained by the other methods.

The strain measurements reported here are qualitatively similar to those reported in the ceramic²⁴ 90% $\text{Pb}(\text{Mg}_{1/3}\text{Nb}_{2/3})\text{O}_3$ -10% PbTiO_3 . In this ceramic material, the high-temperature region (above $\approx 300^\circ\text{C}$) can be approximated by linear behavior and very little happens at T_c ($\approx 50^\circ\text{C}$).

In two ferroelectric systems that show a higher-temperature polarization phase similar to that discussed here, the values of T_d could be quantitatively understood in terms of T_c of the end member. For example, T_d of La doped lead zirconate titanate (PLZT) is approximately equal to T_c of lead zirconate titanate (PZT) (Ref. 8) (i.e., La-free material). Similarly, T_d of $\text{Pb}(\text{Ti}_{1-x}\text{Sn}_x)\text{O}_3$ is found¹² to be equal to T_c of PbTiO_3 . For BSN crystals there is no end member for which an estimate of T_d can be made. However, we emphasize that the difference between T_d and T_c is large ($> 200^\circ\text{C}$).

Thus, it seems that at $\approx T_d$ small local regions of the crystal begin to show a polarization due to a favorable arrangement of the atoms (presumably the Ba and Sr atoms). The macroscopic index of refraction and strain measurements can detect this effect because P_d^2 rather than P_d contributes to these terms. These macroscopic measurements average the inhomogeneous contributions, as discussed. Once local regions of polarization occur, the cooperative effect that occurs at T_c can be understood.¹²

A critical question which must be addressed, using supplemental data and experiments, is whether the polarization observed here at temperatures above the weak-field dielectric maximum (T_c) is static, or whether the vector direction in each polar region is suffering dynamical inversions over time. Since both the optical and the dilatometric measurements discussed in this paper measure the rms polarization, either model would give equivalent values for P_d . In general, one would expect that dynamical inversion of P_d in polar micro regions would be modulated by a weak external E_3 field so as to change the fraction of up and down polarizations and thus contribute a significant component to the dielectric polarizability. On the dynamical model, the dielectric peak at T_c in BSN

could occur either due to cooperative ordering of the polar microregions, or to a critical slowing down of the dipolar component of the polarizability and a freezing in of the dipoles to a glass state.

In the static model the dipolar component which appears at temperatures well above T_c is already frozen. Polarizability would now be contributed by expansion and contraction of the dipolar region and the maximum in ϵ_3 and T_c would be essentially due to cooperative ordering.

Lead magnesium niobate ($\text{PbMg}_{1/3}\text{Nb}_{2/3}\text{O}_3$) and lead lanthanum zirconate titanate (PLZT) compositions such as the 8:65:35 show very strong dielectric relaxation for temperatures at and below the weak-field dielectric peak.^{23,24} These materials show a remanent polar state that is only stable at temperatures much below the dielectric peak (the so-called β - α transition in PLZT). In these materials there is rather strong ancillary evidence for the dynamical model.

In BSN 40:60 there is clearly a highly dispersive microdomain state in virgin crystals cooled below 88°C , but, upon poling, stable macrodomains are retained up to 88°C .²⁵ Some evidence for the dynamical model may be adduced from the work of Sundius,²⁶ who measured the electrostrictive Q_{33} , Q_{13} , and Q_{11} constants under alternating field. She finds that Q_{11} is essentially independent of temperature to T_c , but Q_{33} and Q_{31} are markedly temperature dependent and approach zero near T_c . If, as suggested above, a major component of polarizability comes from the flipping of already polar regions, as is evidenced from the dilatometric studies, the lattice has already adjusted dimension for these polar regions and the phenomenon of electrostriction (which is quadratic inversion of P) will not change the crystal shape at all, so that if polar flipping is the major contributor to dielectric polarizability at T_c , Q_{33} and Q_{31} must go to zero at that temperature. For a field E , on the other hand, the up and down states of P_3 will not be affected and "normal" electrostriction constants should be observed.

Another critical experiment which should be attempted is measurement of the quadratic electro-optic constants g_{33} , g_{13} , and g_{11} . If g_{33} and g_{13} approach zero near T_c with the same shape as Q_{33} and Q_{13} , and g_{11} is also temperature independent, further strong support would be provided for the dynamical model.

Perhaps the final key to understanding these fascinating materials will be the identification of the size, shape, and nature of the polar nanostructure using high-resolution transmission-electron microscopy (TEM). Such evidence is now appearing for PLZT's, $\text{PbMg}_{1/3}\text{Nb}_{2/3}\text{O}_3$, and $\text{PbSc}_{1/2}\text{Ta}_{1/2}\text{O}_3$ relaxor ferroelectrics,²⁷⁻²⁹ and will certainly also be important in the BSN compositions.

¹M. E. Lines and A. M. Glass, *Principles and Applications of Ferroelectrics and Related Materials* (Clarendon, Oxford, 1977); F. Jona and G. Shirane, *Ferroelectric Crystals* (Pergamon, New York, 1962).

²S. C. Abrahams, P. B. Jamieson, and J. L. Bernstein, *J. Chem. Phys.* **54**, 2355 (1971), and the references quoted there to their earlier papers.

³G. Burns, *Solid State Physics* (Academic, New York, 1985).

⁴B. A. Scott, E. A. Giess, B. L. Olson, G. Burns, A. W. Smith, and D. F. O'Kane, *Mater. Res. Bull.* **5**, 47 (1970).

⁵K. Megumi, N. Nagatsuma, K. Kashiwada, and Y. Furuhashi, *Mater. Sci.* **11**, 1583 (1976).

⁶R. R. Neurgaonkar, M. H. Kalisher, T. C. Lim, E. J. Staples, and K. K. Keester, *Mater. Res. Bull.* **15**, 1235 (1980); R. R.

- Neurgaonkar, W. K. Cory, and J. R. Oliver, *Ferroelectrics* **15**, 3 (1983).
- ⁷R. R. Neurgaonkar and W. K. Cory, *J. Opt. Soc. Am.* **3**, 274 (1986).
- ⁸G. Burns and F. H. Dacol, *Jpn. J. Appl. Phys.* **24**, Suppl. **24-2**, 85 (1986).
- ⁹G. Burns and F. H. Dacol, *Solid State Commun.* **48**, 853 (1983); G. Burns and B. A. Scott, *ibid.* **13**, 423 (1973).
- ¹⁰G. Burns and F. H. Dacol, *Phys. Rev. B.* **30**, 4012 (1984); G. Burns, *ibid.* **13**, 215 (1976).
- ¹¹J. J. DeYoreo, R. O. Pohl, and G. Burns, *Phys. Rev. B* **32**, 5780 (1985). Rather complete references to earlier work are given here. Also see *Jpn. J. Appl. Phys.* **24**, Suppl. **24-2**, 975 (1986).
- ¹²G. Burns and F. H. Dacol, *Solid State Commun.* **58**, 567 (1986).
- ¹³T. Heinz, G. Burns, and N. Halas, *Bull. Am. Phys. Soc.* **31**, 603 (1986).
- ¹⁴G. Burns, *Phase Transitions* **5**, 261 (1985); G. Burns and F. H. Dacol, *Ferroelectrics* **52**, 103 (1983).
- ¹⁵R. L. Byer and C. B. Roundy, *Ferroelectrics* **3**, 333 (1972).
- ¹⁶A. M. Glass, *J. Appl. Phys.* **40**, 4699 (1969).
- ¹⁷J. F. Nye, *Physical Properties of Crystals* (Clarendon, Oxford, 1957).
- ¹⁸E. L. Venturini, E. G. Spenger, P. V. Lenzo, and A. A. Ballman, *J. Appl. Phys.* **39**, 343 (1968).
- ¹⁹G. Burns, F. H. Dacol, J. P. Remeika, and W. Taylor, *Phys. Rev. B* **26**, 2702 (1982); G. Burns and F. H. Dacol, *Jpn. J. Appl. Phys.* **24**, Suppl. **24-2**, 649 (1986).
- ²⁰G. Burns and A. W. Smith, *IEEE J. Quantum Electron.* **QE-4**, 584 (1968).
- ²¹J. E. Geusic, S. K. Kurtz, L. G. Van Uitert, and S. H. Wemple, *Appl. Phys. Lett.* **4**, 141 (1964).
- ²²M. DiDomenico and S. H. Wemple, *J. Appl. Phys.* **40**, 720 (1969).
- ²³L. E. Cross, S. J. Jang, R. E. Newnham, S. Nomura, and K. Uchino, *Ferroelectrics* **23**, 187 (1980).
- ²⁴Y. Xi, C. Z. Li, and L. E. Cross, *J. Appl. Phys.* **54**, 3399 (1983).
- ²⁵T. W. Cline, Ph.D. thesis, The Pennsylvania State University, 1977.
- ²⁶C. Sundius, M. Sc. thesis, The Pennsylvania State University, 1983.
- ²⁷M. P. Harmer, A. S. Bhalla, B. H. Fox, and L. E. Cross, *Mater. Lett.* **2**, 278 (1984).
- ²⁸H. M. Chan, M. P. Harmer, A. S. Bhalla, and L. E. Cross, *Jpn. J. Appl. Phys.* **24**, 550 (1985).
- ²⁹H. M. Chan, M. P. Harmer, A. S. Bhalla, and L. E. Cross, *Am. Ceram. Soc. Bull.* **65**, 517 (1986).